Graphene

Deutsche Ausgabe: DOI: 10.1002/ange.201605457
Internationale Ausgabe: DOI: 10.1002/anie.201605457

Functionalization of Hydrogenated Graphene: Transition-Metal-Catalyzed Cross-Coupling Reactions of Allylic C–H Bonds

*Chun Kiang Chua, Zdeněk Sofer, and Martin Pumera**

Abstract: *The chemical functionalization of hydrogenated graphene can modify its physical properties and lead to better processability. Herein, we describe the chemical functionalization of hydrogenated graphene through a dehydrogenative cross-coupling reaction between an allylic C–H bond and the α-C–H bond of tetrahydrothiophen-3-one using $Cu(OTf)_2$ as the catalyst and DDQ as the oxidant. The chemical functionalization was confirmed by X-ray photoelectron spectroscopy and Fourier transform infrared spectroscopy and visualized by scanning electron microscopy. The functionalized hydrogenated graphene material demonstrated improved dispersion stability in water, bringing new quality to the elusive hydrogenated graphene (graphane) materials. Hydrogenated graphene provides broad possibilities for chemical modifications owing to its reactivity.*

Chemical functionalization offers a multitude of opportunities to develop functional graphene materials. It is known that the chemical functionalization of graphene can permanently alter its electronic structure and electrical and physical properties.[1] Numerous functionalization strategies, including nucleophilic addition,[2] cycloaddition,[3] free radical addition,[4] substitution,[5] and rearrangement[6] reactions, have been demonstrated over the last five years to improve the processability and modify the band gap of graphene. In addition, functionalization with heteroatoms such as boron,[7] nitrogen,[8] and sulfur[9] directly onto the sp^2 carbon atoms of graphene has also improved the versatility of graphene. Chemical functionalization has enabled the extensive usage of graphene in various applications ranging from supercapacitors,[10] photovoltaic devices,[11] and energy production[9a] to sensing devices.[12] Hydrogenation is a direct strategy to engineer the band gap of graphene in a controllable and reversible manner.[13] Hydrogenated graphene (graphane) demonstrates a myriad of interesting properties, such as fluorescence and ferromagnetism,[14] and would naturally find its applications in two-dimensional electronics and as a hydrogen storage material.[13a]

[*] Dr. C. K. Chua, Prof. M. Pumera
Division of Chemistry and Biological Chemistry
School of Physical and Mathematical Science
Nanyang Technological University
21 Nanyang Link, Singapore 637371 (Singapore)
E-mail: pumera.research@gmail.com
Prof. Z. Sofer
University of Chemistry and Technology Prague
Department of Inorganic Chemistry
Technická 5, 166 28 Prague 6 (Czech Republic)

Supporting information for this article can be found under: http://dx.doi.org/10.1002/anie.201605457.

Graphene hydrogenation produces predominantly $C(sp^3)$–H bonds, which renders it chemically inert and limits its usefulness in more complex applications. Chemical functionalization could hence introduce active functional groups onto hydrogenated graphene through C–C bond formation, as demonstrated by the grafting of a diazonium salt in a free radical reaction.[15] It should be mentioned that experimentally obtained hydrogenated graphene exhibits various regions of different conformational isomers (i.e., chair, boat, twist-boat, and twist-boat-chair)[16] as well as islands of sp^2 bonded carbon atoms. Such a chemical structure suggests the widespread presence of allylic C–H bonds, which can function as active precursors for chemical functionalization.[15]

We herein present an allylic C–H bond functionalization strategy for bulk hydrogenated graphene. The functionalization is based on a dehydrogenative cross-coupling reaction between allylic C–H bonds of hydrogenated graphene and the α-C–H bonds of ketones using $Cu(OTf)_2$ as the catalyst and DDQ as the oxidant (Scheme 1).[17]

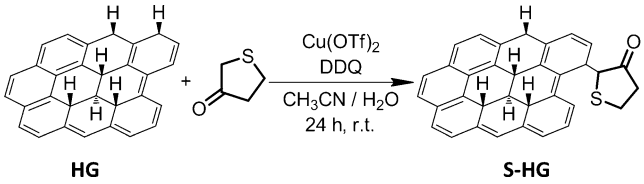

Scheme 1. Cross-coupling reaction between hydrogenated graphene and tetrahydrothiophen-3-one.

Hydrogenated graphene (HG) was obtained by the simultaneous reduction and hydrogenation of graphene oxide according to the Birch reduction method.[18] The dehydrogenative cross-coupling reaction occurred between an allylic C–H bond of hydrogenated graphene and an α-C–H bond of tetrahydrothiophen-3-one (THT) to provide THT-functionalized hydrogenated graphene (S-HG). A control experiment (HG-C) was performed with hydrogenated graphene in a mixture containing only THT to examine the possible adsorption of THT onto the surface of hydrogenated graphene. The hydrogenated graphene materials were subsequently analyzed by X-ray photoelectron spectroscopy (XPS), Fourier transform infrared (FTIR), and scanning electron microscopy energy dispersive X-ray spectroscopy (SEM-EDS).

The chemical functionalization was carefully examined with XPS, a surface-sensitive analysis technique. Figure 1 A shows survey scans of HG, S-HG, and HG-C. HG consisted primarily of the elements oxygen and carbon. Upon function-

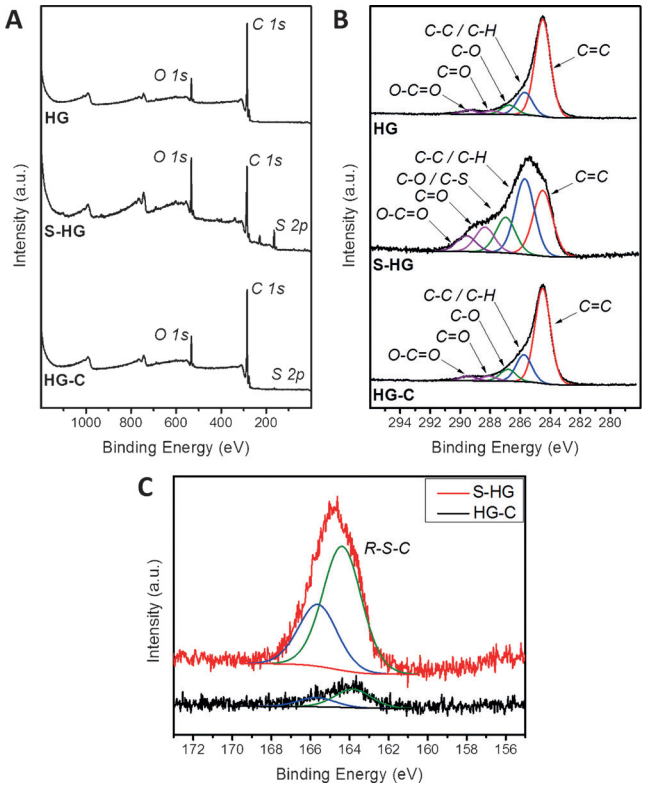

Figure 1. A) Survey and B) C 1s core-level XPS spectra for HG, S-HG, and HG-C. C) S 2p core-level spectra for S-HG and HG-C.

alization, sulfur was detected in S-HG at up to 8.8 at%. On the other hand, the 0.8 at% of sulfur that were detected for HG-C suggest the possible adsorption of THT onto HG. The amounts of copper, chlorine, and fluorine originating from trace $Cu(OTf)_2$ and DDQ were below the detection limit of XPS.

To gain more insight into the functionalization, C 1s core-level spectra were recorded (Figure 1B). The C 1s core-level spectra were deconvoluted into five components at binding energies of 284.5 (C=C), 285.7 (C–C and C–H), 286.9 (C–O), 288.3 (C=O), and 289.6 eV (O–C=O).[18,19] The intense C=C peak in HG suggested that many allylic C–H bonds would be present for functionalization. This was further supported by the peak at 285.7 eV, which indicated the presence of C–C and C–H bonds (see below for the FTIR analysis). Following the functionalization to afford S-HG, the peak intensities at 285.7 and 286.9 eV increased. The increase in the former peak suggests an increased number of C–C and C–H bonds as a result of the covalently attached THT molecules. On the other hand, the increase in the intensity of the latter peak could be attributed to the presence of C–S bonds, although their binding energies usually fall within the range of 285 to 287 eV.[9b,20] Nevertheless, the higher number of C=O bonds found in S-HG served as a strong indicator for the successful functionalization of HG with THT. The increased peak intensities of these components cannot be due to the adsorption of THT on HG as the C 1s core-level spectrum of HG-C closely resembled that of HG. Subsequently, the S 2p core-level spectra of S-HG and HG-C, as shown in Figure 1C, were split into spin–orbit doublets of S $2p_{3/2}$ and S $2p_{1/2}$ at 164.3 and 165.6 eV, respectively, which represents sulfur bonding of the R–S–C type. The differences in the S 2p peak intensities of S-HG and HG-C further served as evidence for the extent and success of the functionalization of HG with THT.

Scanning electron spectroscopy/energy-dispersive X-ray spectroscopy (SEM-EDS) analysis was subsequently performed to support the findings from the XPS analysis. As EDS analysis provides a higher depth of analysis and detection limit, the bulk properties of S-HG can be determined. Based on the SEM images (see the Supporting Information, Figure S1), HG displayed characteristic wrinkled surfaces owing to the expansion of the hydrogenated sheets. In comparison, even though S-HG and HG-C displayed wrinkled surfaces, stacked morphologies could be observed. This finding suggested possible sheet aggregation induced by the chemical treatment. Initial EDS analysis on HG indicated the presence of only carbon and oxygen species (see Figure S2). On the other hand, sulfur was detected at 4.9 at% on S-HG (Figure 2). Traces of copper, chlorine, and fluorine were detected at comparatively low levels (ca. 0.3 at%) owing to possible adsorption. For HG-C, the amount of sulfur detected (0.3 at%) was relatively low compared to that in S-HG (Figure S3). This is consistent with the findings from XPS analysis.

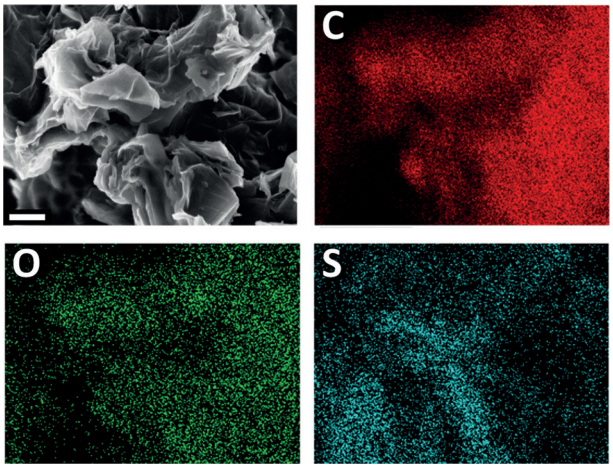

Figure 2. SEM-EDS analysis of S-HG. Scale bar: 1 μm.

The functionalization of hydrogenated graphene with THT will inevitably modify the amount of C–H and C=O functional groups, and these changes can be monitored by FTIR spectroscopy. The FTIR spectra of HG, S-HG, and HG-C are shown in Figure 3. At first glance, the spectrum of HG was similar to that of HG-C, and a strong absorption at about 2900 cm^{-1}, which corresponds to C–H stretching, was observed. This result indicates that THT, in the absence of $Cu(OTf)_2$ and DDQ, did not undergo any chemical reaction with the C–H groups on hydrogenated graphene. However, the spectrum of S-HG showed a decrease in the absorbance for C–H stretching. This suggested a depletion of C–H groups in S-HG, which would otherwise give rise to an intense C–H

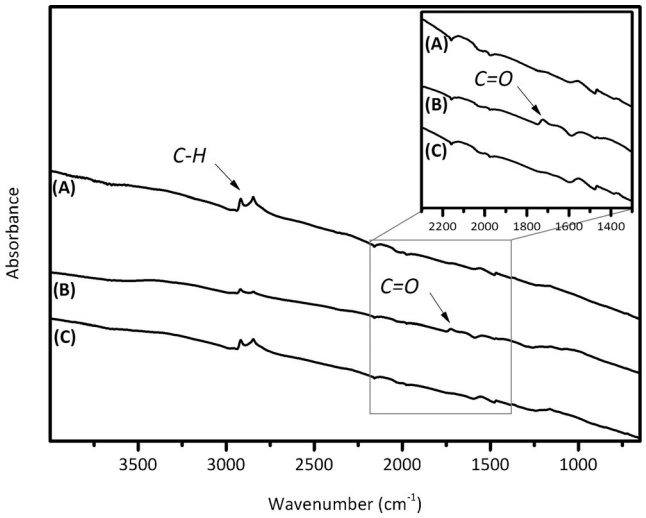

Figure 3. FTIR spectra of A) HG, B) S-HG, and C) HG-C. The inset shows an expanded view of the indicated region.

stretching band as seen for HG and HG-C. In fact, the C–H stretching observed for S-HG could also be correlated with the presence of covalently attached THT molecules. This was further supported by the evolution of a C=O stretching band (at ca. 1720 cm^{-1}), which was only present in S-HG (Figure 3, inset).

Despite these structural and morphological characterizations, the effect of functionalization can best be demonstrated by changes in the physical properties of the materials, especially in terms of the dispersion stability. As hydrogenated graphene is expected to consist predominantly of C–H groups, its dispersion stability in water should be very poor. This was indeed the case, and HG appeared to float on the surface of water (Figure 4). As anticipated from earlier analyses, HG-C showed similar hydrophobic characteristics to HG. On the other hand, S-HG dispersed well in water to form a gray dispersion. The improved dispersion stability is most likely due to the presence of moderately polar C=O functional groups in S-HG, which promote hydrogen-bonding interactions with water molecules.

In a separate investigation that utilized cyclohexanone as the α-C–H bond component for functionalization, the resulting cyclohexanone-functionalized hydrogenated graphene (Cy-HG) showed low dispersion stability in water. Further XPS and FTIR analyses did not provide any indications that chemical functionalization had been successful (see Figure S4). More importantly, these observations with Cy-HG also indicate the low likelihood of adsorbed $Cu(OTf)_2$ and DDQ promoting the dispersion of hydrogenated graphene in water.

In summary, we have demonstrated that hydrogenated graphene can be functionalized through allylic C–H functionalization. The feasibility of the functionalization was supported by XPS, SEM-EDS, and FTIR analysis. Future work could investigate the installation of possible side-group derivatives on THT or introduce other functional groups to tune the optical and physical properties of hydrogenated graphene.

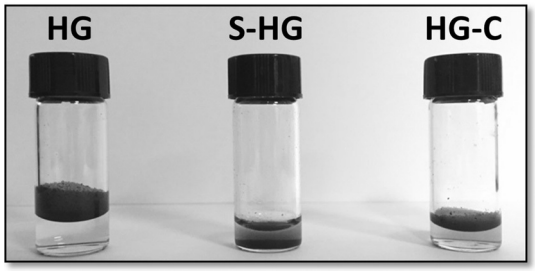

Figure 4. Photographs of HG, S-HG, and HG-C dispersions. Dispersions of 1 mg mL^{-1} in ultrapure water after ultrasonication for 10 min are shown.

Experimental Section

The method for the preparation of hydrogenated graphene has already been reported.[18] $Cu(OTf)_2$ (27 mg) was added into acetonitrile (5 mL) at 0 °C. Subsequently, hydrogenated graphene (3 mg), tetrahydrothiophen-3-one (THT; 256 μL) or cyclohexanone (310 μL), and H_2O (40.5 μL) were added in this order. 2,3-Dichloro-5,6-dicyano-1,4-benzoquinone (DDQ; 340 mg) was then added in three portions over 1.5 h. The reaction mixture was left to stir for 24 h at room temperature. It was then filtered and washed over a PTFE membrane (0.2 μm pore size) with water and methanol. The filtered black solid was withdrawn at three separate intervals, dispersed in a mixture of methanol/water, and subjected to ultrasonication (180 W, 2 min). The filtered black solid was dried in a vacuum oven at 40 °C for 5 days prior to usage.

X-ray photoelectron spectroscopy was performed with a Phoibos 100 spectrometer and a Mg X-ray radiation source (SPECS, Germany). Both survey and high-resolution spectra were collected for C 1s and S 2p. Relative sensitivity factors were used for evaluating the atomic percentages from the XPS survey spectra. XPS samples were prepared by coating a carbon tape with a uniform layer of the graphene material under study. A JEOL JSM-7600F semi-in-lens FE-SEM was used to acquire the SEM images. The graphene materials were transferred to a carbon tape held onto a SEM holder for analysis. EDS data were obtained using an Oxford instrument and analyzed using the Aztec software. ATR-FTIR measurements were carried out on a PerkinElmer Spectrum 100 system with a universal ATR accessory.

Acknowledgements

This work was supported by a Tier 2 grant (MOE2013-T2-1-056; ARC 35/13) from the Ministry of Education, Singapore. Z.S. was supported by the Czech Science Fundation (GACR No. 15-09001S).

Keywords: cross-coupling · graphene · heterogeneous catalysis · hydrogenated graphene · transition metals

How to cite: *Angew. Chem. Int. Ed.* **2016**, *55*, 10751–10754
Angew. Chem. **2016**, *128*, 10909–10912

[1] a) K. P. Loh, Q. Bao, P. K. Ang, J. Yang, *J. Mater. Chem.* **2010**, *20*, 2277–2289; b) V. Georgakilas, M. Otyepka, A. B. Bourlinos, V. Chandra, N. Kim, K. C. Kemp, P. Hobza, R. Zboril, K. S. Kim, *Chem. Rev.* **2012**, *112*, 6156–6214; c) E. Bekyarova, S. Sarkar, F. Wang, M. E. Itkis, I. Kalinina, X. Tian, R. C. Haddon, *Acc.*

Chem. Res. **2013**, *46*, 65 – 76; d) C. K. Chua, M. Pumera, *Chem. Soc. Rev.* **2013**, *42*, 3222 – 3233; e) Q. Tang, Z. Zhou, Z. Chen, *Nanoscale* **2013**, *5*, 4541 – 4583; f) L. Liao, H. Peng, Z. Liu, *J. Am. Chem. Soc.* **2014**, *136*, 12194 – 12200; g) A. Bellunato, H. Arjmandi Tash, Y. Cesa, G. F. Schneider, *ChemPhysChem* **2016**, *17*, 785 – 801.

[2] S. P. Economopoulos, G. Rotas, Y. Miyata, H. Shinohara, N. Tagmatarchis, *ACS Nano* **2010**, *4*, 7499 – 7507.

[3] a) J. Choi, K.-J. Kim, B. Kim, H. Lee, S. Kim, *J. Phys. Chem. C* **2009**, *113*, 9433 – 9435; b) S. Sarkar, E. Bekyarova, S. Niyogi, R. C. Haddon, *J. Am. Chem. Soc.* **2011**, *133*, 3324 – 3327; c) C. K. Chua, A. Ambrosi, M. Pumera, *Chem. Commun.* **2012**, *48*, 5376 – 5378; d) J. Li, M. Li, L.-L. Zhou, S.-Y. Lang, H.-Y. Lu, D. Wang, C.-F. Chen, L.-J. Wan, *J. Am. Chem. Soc.* **2016**, *138*, 7448 – 7451.

[4] a) J. R. Lomeda, C. D. Doyle, D. V. Kosynkin, W. F. Hwang, J. M. Tour, *J. Am. Chem. Soc.* **2008**, *130*, 16201 – 16206; b) H. Liu, S. Ryu, Z. Chen, M. L. Steigerwald, C. Nuckolls, L. E. Brus, *J. Am. Chem. Soc.* **2009**, *131*, 17099 – 17101.

[5] a) C. K. Chua, M. Pumera, *Chem. Asian J.* **2012**, *7*, 1009 – 1012; b) C. Yuan, W. Chen, L. Yan, *J. Mater. Chem.* **2012**, *22*, 7456 – 7460.

[6] W. R. Collins, W. Lewandowski, E. Schmois, J. Walish, T. M. Swager, *Angew. Chem. Int. Ed.* **2011**, *50*, 8848 – 8852; *Angew. Chem.* **2011**, *123*, 9010 – 9014.

[7] S. Agnoli, M. Favaro, *J. Mater. Chem. A* **2016**, *4*, 5002 – 5025.

[8] H. Wang, T. Maiyalagan, X. Wang, *ACS Catal.* **2012**, *2*, 781 – 794.

[9] a) Z. Yang, Z. Yao, G. Li, G. Fang, H. Nie, Z. Liu, X. Zhou, X. Chen, S. Huang, *ACS Nano* **2011**, *6*, 205 – 211; b) C. K. Chua, M. Pumera, *ACS Nano* **2015**, *9*, 4193 – 4199.

[10] a) H. M. Jeong, J. W. Lee, W. H. Shin, Y. J. Choi, H. J. Shin, J. K. Kang, J. W. Choi, *Nano Lett.* **2011**, *11*, 2472 – 2477; b) Z. Lei, J. Zhang, L. L. Zhang, N. A. Kumar, X. S. Zhao, *Energy Environ. Sci.* **2016**, *9*, 1891 – 1930.

[11] Z. Liu, S. P. Lau, F. Yan, *Chem. Soc. Rev.* **2015**, *44*, 5638 – 5679.

[12] a) V. Urbanová, K. Holá, A. B. Bourlinos, K. Čépe, A. Ambrosi, A. H. Loo, M. Pumera, F. Karlický, M. Otyepka, R. Zbořil, *Adv. Mater.* **2015**, *27*, 2305 – 2310; b) K. Ariga, K. Minami, L. K. Shrestha, *Analyst* **2016**, *141*, 2629 – 2638.

[13] a) J. O. Sofo, A. S. Chaudhari, G. D. Barber, *Phys. Rev. B* **2007**, *75*, 153401; b) D. C. Elias, R. R. Nair, T. M. G. Mohiuddin, S. V. Morozov, P. Blake, M. P. Halsall, A. C. Ferrari, D. W. Boukhvalov, M. I. Katsnelson, A. K. Geim, K. S. Novoselov, *Science* **2009**, *323*, 610 – 613; c) R. Balog, B. Jørgensen, L. Nilsson, M. Andersen, E. Rienks, M. Bianchi, M. Fanetti, E. Laegsgaard, A. Baraldi, S. Lizzit, Z. Sljivancanin, F. Besenbacher, B. Hammer, T. G. Pedersen, P. Hofmann, L. Hornekær, *Nat. Mater.* **2010**, *9*, 315 – 319.

[14] a) J. Zhou, Q. Wang, Q. Sun, X. S. Chen, Y. Kawazoe, P. Jena, *Nano Lett.* **2009**, *9*, 3867 – 3870; b) R. A. Schäfer, J. M. Englert, P. Wehrfritz, W. Bauer, F. Hauke, T. Seyller, A. Hirsch, *Angew. Chem. Int. Ed.* **2013**, *52*, 754 – 757; *Angew. Chem.* **2013**, *125*, 782 – 786.

[15] Z. Sun, C. L. Pint, D. C. Marcano, C. Zhang, J. Yao, G. Ruan, Z. Yan, Y. Zhu, R. H. Hauge, J. M. Tour, *Nat. Commun.* **2011**, *2*, 559.

[16] D. K. Samarakoon, X.-Q. Wang, *ACS Nano* **2009**, *3*, 4017 – 4022.

[17] X.-F. Huang, M. Salman, Z.-Z. Huang, *Chem. Eur. J.* **2014**, *20*, 6618 – 6621.

[18] A. Y. S. Eng, Z. Sofer, Š. Huber, D. Bouša, M. Maryško, M. Pumera, *Chem. Eur. J.* **2015**, *21*, 16828 – 16838.

[19] M. Pumera, C. H. A. Wong, *Chem. Soc. Rev.* **2013**, *42*, 5987 – 5995.

[20] a) H. L. Poh, P. Šimek, Z. Sofer, M. Pumera, *ACS Nano* **2013**, *7*, 5262 – 5272; b) H. R. Thomas, A. J. Marsden, M. Walker, N. R. Wilson, J. P. Rourke, *Angew. Chem. Int. Ed.* **2014**, *53*, 7613 – 7618; *Angew. Chem.* **2014**, *126*, 7743 – 7748.

Received: June 5, 2016
Revised: July 7, 2016
Published online: August 5, 2016

